

Ultra-Wide-Field Fluorescein Angiography–Guided Normalization of Ischemic Index Calculation in Eyes With Retinal Vein Occlusion

Kang Wang,^{1–3} Khalil Ghasemi Falavarjani,^{1,2,4} Muneeswar G. Nittala,¹ Min Sagong,⁵ Charles C. Wykoff,⁶ Jano van Hemert,⁷ Michael Ip,^{1,2} and Srinivas R. Sadda^{1,2}

¹Doheny Image Reading Center, Doheny Eye Institute, Los Angeles, California, United States

²Department of Ophthalmology, David Geffen School of Medicine at UCLA, Los Angeles, California, United States

³Department of Ophthalmology, Beijing Friendship Hospital, Capital Medical University, Beijing, China

⁴Eye Research Center and Eye Department, Rassoul Akram Hospital, Iran University of Medical Sciences, Tehran, Iran

⁵Department of Ophthalmology, Yeungnam University College of Medicine, Daegu, South Korea

⁶Blanton Eye Institute & Houston Methodist Hospital, Houston, Texas, United States

⁷Optos PLC, Dunfermline, United Kingdom.

Correspondence: Srinivas R. Sadda, Doheny Eye Institute, PO Box 86228, Los Angeles, CA 90086, USA; ssadda@doheny.org.

Submitted: January 4, 2018

Accepted: June 6, 2018

Citation: Wang K, Ghasemi Falavarjani K, Nittala MG, et al. Ultra-wide-field fluorescein angiography–guided normalization of ischemic index calculation in eyes with retinal vein occlusion. *Invest Ophthalmol Vis Sci.* 2018;59:3278–3285. <https://doi.org/10.1167/iivs.18-23796>

PURPOSE. The purpose of this study was to compare the use of central and montaged ultra-wide-field fluorescein angiography (UWFFA) images for calculating the area of nonperfusion (NP) and ischemic index (ISI) in patients with retinal vein occlusion (RVO) and macular edema (ME) and to correlate these measurements with best-corrected visual acuity (BCVA) and central macular thickness (CMT).

METHODS. Thirty eyes of 30 RVO patients with recurrent ME were enrolled. Baseline UWFFA images were sent to the Doheny Image Reading Center for quantitative analysis by certified graders. The association between ISI from the various zones and BCVA and CMT was examined by Spearman rank correlation and compared. Generalized linear models (GLMs) were used to analyze associations between BCVA and disease status.

RESULTS. The NP area and ISI for central and montaged images were not significantly different for any retinal zone. A modest but statistically significant negative linear correlation was observed between BCVA and ISI, ranging from $r = -0.3825$ in the perimacular area (PMA) to $r = -0.584$ in the far peripheral area (FPA). On GLM analysis, both PMA ($\beta = -1.059$; 95% confidence interval: -1.74 to -0.378) and FPA ($\beta = -0.505$; 95% confidence interval: -0.988 to -0.021) were significant independent predictors of BCVA. We found no correlation between ISI from the various zones and CMT in this cohort.

CONCLUSIONS. Montaging of UWFFA images may not be required to adequately quantify and represent areas of NP in eyes with RVO. NP in both the PMA and peripheral retina appear relevant to visual function, highlighting the importance of evaluating the retinal periphery in these individuals.

Keywords: ischemic index, ultra-wide field, retinal vein occlusion, macular edema

Retinal vein occlusion (RVO) is a common cause of visual loss in patients with hypertension, diabetic retinopathy, ischemic heart disease, and hypercholesterolemia.¹ Visual loss secondary to RVO is often caused by macular edema (ME), which is thought to be related to ischemic nonperfusion (NP) of the retina and subsequent leakage of abnormal vasculature. The retinal NP in eyes with RVO can vary greatly and involve large regions of the peripheral retina.² The extent of nonperfusion has been shown to affect the risk of developing neovascularization, as well as the severity of ME.^{2–4} Current ultra-wide-field fluorescein angiography (UWFFA) devices allow capture of a single, high-resolution, “200-degree” image of the retinal area, covering more than 80% of the retinal surface, with all vessels displayed in the same angiographic phase.⁵ The recent introduction of stereographic projection software to correct for inherent peripheral distortion has allowed precise

and accurate measurement of peripheral lesions including the retinal NP area.^{4,6}

The ischemic index (ISI), a ratio of nonperfused retina to total visible retina, has predictive/prognostic value.⁵ Accurately assessing the NP area and the total area of visible retina to generate the ISI, however, can be challenging.^{2,7–9} The far periphery, especially superiorly and inferiorly, may not always be clearly seen on a central/on-axis ultra-wide-field (UWF) image. Lash artifact can further exacerbate the problem. Montaging steered images can mitigate this problem; however, the component images will not be in precisely the same phase of the angiogram. In addition, when judging the significance of areas of nonperfusion, one needs to consider that a normal avascular zone (physiologic nonperfusion) exists in the far retinal periphery.^{10,11} Moreover, the total area of the visible retina may vary greatly from patient to patient, or even for the same patient at different visits. There are questions as to



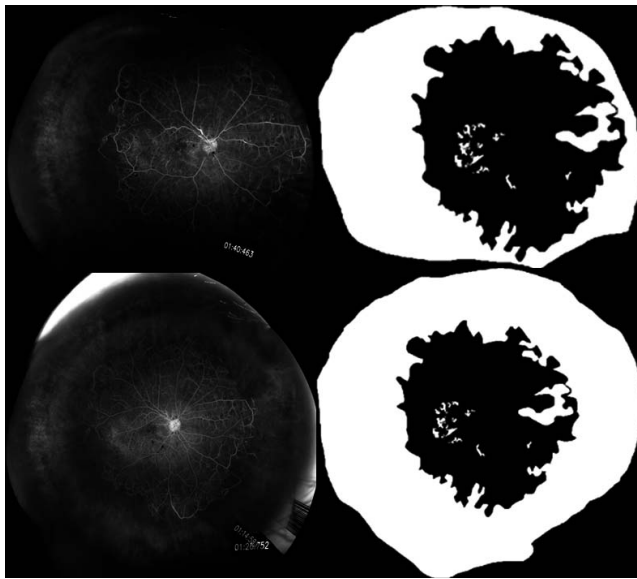


FIGURE 1. UWFFA image of an eye with retinal vein occlusion: single central image versus montaged image. Illustration of central and montaged images (*top left, bottom left*) with binary masks (*top right, bottom right*) for a patient with retinal central vein occlusion. The *white regions* demarcate areas of nonperfusion in the binary images.

whether these variations may lead to errors in calculating the ISI and whether using montaged images with a clearer view of the peripheral visible retina will allow more accurate calculation of ISI.

For the present study, we sought to compare the use of central and montaged UWFFA images for calculating the NP area and ISI in patients with ischemic RVO and persistent ME enrolled in the WAVE trial (widefield angiography-guided targeted-retinal photocoagulation combined with anti-VEGF intravitreal injections for the treatment of ischemic central retinal vein occlusion, hemi retinal vein occlusion, and branch retinal vein occlusion).

METHODS

Study Population

The WAVE study (NCT 01710839) is a phase IV, prospective clinical trial of patients with persistent ME associated with ischemic RVO, despite treatment with anti-VEGF. Subjects in the WAVE study were randomized to receive either ranibizumab monotherapy or combination ranibizumab and targeted retinal laser photocoagulation (TRP) to areas of peripheral NP. Subjects were recruited from the Retina Consultants of Houston (Houston, Katy, and Woodlands, Texas), and the research was approved by the local Institutional Review Board. This study was performed in accordance with the Health Insurance Portability and Accountability Act and adhered to the tenets of the Declaration of Helsinki. Written informed consent was obtained from all subjects before enrollment.

Major eligibility criteria included the following: age > 18 years; best-corrected visual acuity (BCVA) between 20/25 and 20/800 (between 8 and 61 Early Treatment Diabetic Retinopathy Study [ETDRS] letters); central macular thickness (CMT) ≥ 300 μm due to ME; at least two previous consecutive monthly injections of anti-VEGF therapy with evidence of persistent or recurrent ME; and retinal NP outside of the arcades on screening UWFFA amenable to laser photocoagulation.

In addition to UWFFA, all subjects underwent detailed clinical examinations, including autorefractometry, BCVA, IOP measurement, slit-lamp examination, ophthalmoscopy, and optical coherence tomography (Spectralis Heidelberg Retina Angiograph [HRA]+ optical coherence tomography [OCT]; Heidelberg Engineering, Heidelberg, Germany).

Acquisition of UWFFA Image

UWFFA was performed at screening using an Optos 200Tx instrument (Optos, Dunfermline, UK) with a standardized protocol. After dilation, UWF pseudocolor images were captured centered on the fovea of the study eye. After intravenous administration of fluorescein dye, central images (centered on the fovea) were obtained during the early (45 seconds), middle (2 minutes and 30 seconds), and late (5 minutes) phases of the angiography. After the early phase, additional images were obtained by steering superiorly, inferiorly, temporally, and nasally in the mid and late phases. From our previous studies, the mid-phase images were deemed most critical for delineating areas of nonperfusion.

All images were exported and sent to the Doheny Image Reading Center, Doheny Eye Institute, Los Angeles, California, USA, for analysis. UWFFA images were transformed to stereographic projection images using proprietary software available from the manufacturer. The software also allowed automatic registration of the steered images to the central image to create a montaged image.

Quality Control of Image Grading and Quantification

Two trained, reading center-certified ophthalmologists (KW and KGF) independently analyzed the UWFFA images in a masked fashion. A single central image from the late arteriovenous or early mid-phase was selected for manual delineation of areas of NP. The best image was chosen based on the largest field of view and the greatest image clarity. Each grader was free to choose a different image. A montaged image was selected and graded using the same standard, with the grader masked to the analysis of the single central image. The grader was allowed to enhance the images by using the smoothing and optimizing functions, by adjusting contrast, brightness, and gamma, and by zooming.

The definition of NP was adapted from the Standard Care vs Corticosteroid for Retinal Vein Occlusion (SCORE) study with slight modification.¹² Nonperfusion is characterized by the absence of retinal arterioles and/or capillaries and is detected by characteristics such as a pruned appearance of adjacent arterioles and a darker appearance of the background fluorescence; potential zones of NP with a diameter <500 μm were not delineated.

Using ImageJ version 1.49b (National Institutes of Health, Bethesda, MD, USA), graders manually outlined the NP area and the peripheral extent of total visible retinal area. Grading results were saved as binary masks (Fig. 1) and subsequently calculated in square millimeters by summing the size of all pixels that make up the mask using the manufacturer's quantification software. To aid the grader in determining whether a zone of NP was ≥ 500 μm , a custom map composed of 500- μm diameter circles (0.196 mm^2) was created (Fig. 2, left). Such a map is critical as the physical (on the retina) size of the pixels in the periphery is smaller than that of those in the posterior. In addition, we constructed a custom mask/grid (Fig. 2, right) based on the mean vascular border of a normal perfused retina as established in our previous publication.¹⁰ This boundary is important as NP beyond this region would be considered physiologic and not related to the disease process.

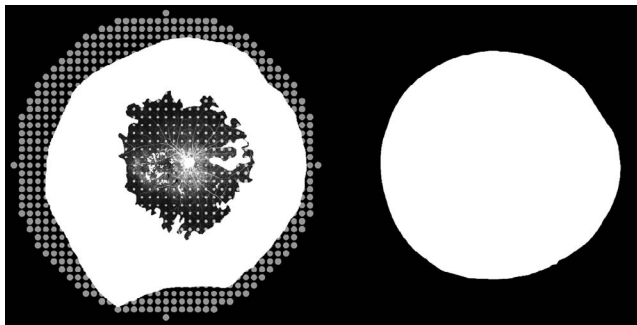


FIGURE 2. To aid the grader in determining whether a zone of NP was $\geq 500 \mu\text{m}$, a custom map composed of $500\text{-}\mu\text{m}$ diameter circles (0.196 mm^2) was created. The manufacturer provided us a custom mask/grid based on the mean vascular border of a normal perfused retina. *Left*, illustration of filled circles $500 \mu\text{m}$ diameter overlaid on a montaged image for nonperfusion area grading reference. *Right*, mask of normal perfusion area.

To assess the amount and severity of NP in different areas, we used a Doheny Image Reading Center standard grid with concentric rings centered on the fovea to define five zones: perimacular area (PMA; 0.5- to 3-mm radius), near-peripheral area (NPA; 3 to 10 mm), mid-peripheral area (MPA; 10 to 15 mm), far-peripheral area (FPA; 15-mm normal perfusion boundary), and the peripheral normal avascular area. The central 1-mm diameter region (foveal central subfield) including the foveal avascular zone was masked and excluded from the NP area. The NP image mask was applied to this grid (Fig. 3), allowing the NP and the ISI (defined as NP divided by the total visible retina within the zone of interest) to be calculated for the various zones.

Statistical Analysis

Statistical analysis of the data was performed using commercial software (version 9.4; SAS Institute, Inc., Cary, NC, USA) and GraphPad Prism 5 (GraphPad Software, Inc., La Jolla, CA, USA). Intraclass correlation coefficients (ICCs) and Bland-Altman plots were used to assess intergrader reproducibility. The mean

of the initial image grading of the two independent graders was used in all subsequent analyses. The Mann-Whitney *U* test was used to compare continuous variables between groups of eyes with branch retinal vein occlusion (BRVO) versus those with central retinal vein occlusion (CRVO), as well as to assess for significant differences between central and montaged groups. We specifically compared the BRVO and CRVO groups as they represent different diseases with different pathophysiologic mechanisms. The χ^2 test was used to compare frequencies of categorical variables as appropriate. A Friedman test was used to compare ISI values from different zones. The Spearman rank correlation was calculated to examine the association between NP and ISI from the various rings/zones and BCVA and CMT. A generalized linear model (GLM) with gamma distribution and log link function was used to estimate the relationship between the BCVA and disease status (as shown with ISI from the various rings/zones) adjusting for age and duration of disease. A stepwise procedure was performed to select independent variable selection. Covariates were decided into the multivariate model via the Schwarz Bayesian information criterion.¹³ A minimum value of $P < 0.05$ was considered statistically significant.

RESULTS

This study included UWFFA images of 30 eyes from 30 patients with BRVO (14 eyes) and CRVO (16 eyes). Mean age of patients 64.1 years (range, 43 to 80 years); 50% were female. Mean baseline BCVA was 53.5 letters, with a mean spherical equivalent of -0.15 diopters (D) (range, -2.50 to $+2.75$ D; $\text{SD} \pm 1.1$ D). Mean baseline CMT was $496.5 \mu\text{m}$. Subjects received an average of 10 intravitreal injections (range, 2 to 41 injections), with an average disease duration of 1.75 years (range, 0 to 7 years).

Reproducibility of NP Grading

Intergrader agreement on the NP area for central and montaged images was excellent, with ICCs ranging from 0.985 to 0.992 and 0.971 to 0.991, respectively (Table 1). The high level of

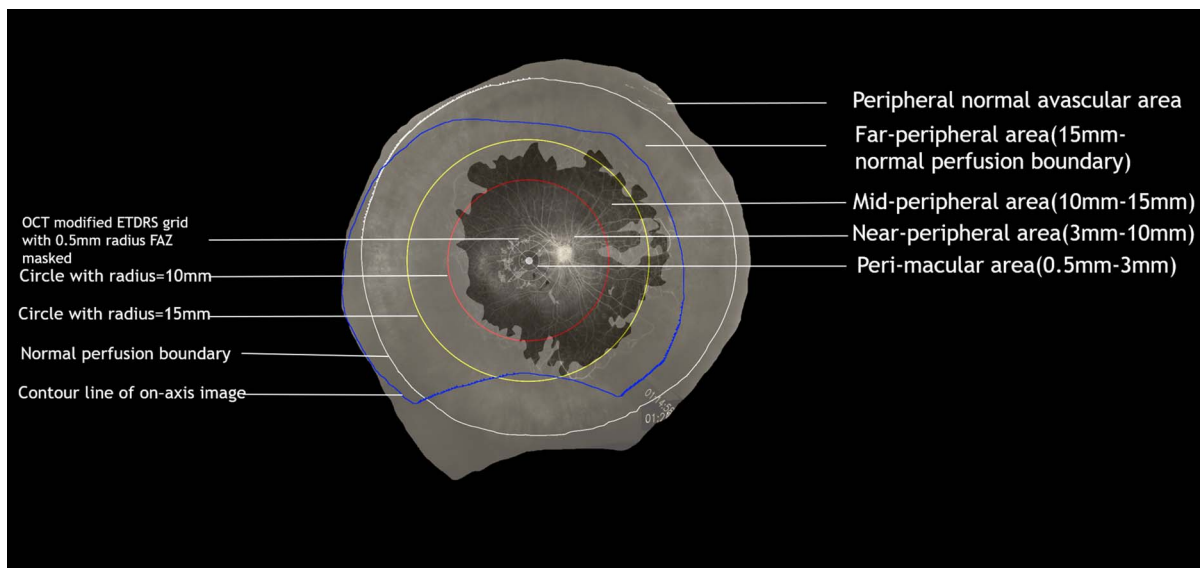


FIGURE 3. A standardized grid with concentric rings centered on the fovea was used to calculate NP and ISI (defined as NP area divided by area of the ring of interest). Definitions based on UWFFA image and zones of determination of retinal nonperfusion shown on montaged image (all centered on the fovea). FAZ, foveal avascular zone.

TABLE 1. Interobserver Reliability of Central and Montaged Image

Variable	ICC (95% CI) Central Image	ICC (95% CI) Montaged Image
PMA	0.988 (0.967-0.995)	0.988 (0.967-0.995)
NPA	0.992 (0.979-0.996)	0.991 (0.979-0.996)
MPA	0.985 (0.969-0.993)	0.983 (0.964-0.992)
FPA	0.985 (0.965-0.993)	0.971 (0.924-0.987)
TA within NPB	0.988 (0.96-0.995)	0.987 (0.963-0.995)
TA of visible retina	0.989 (0.971-0.997)	0.983 (0.932-0.994)

agreement between the two graders is also illustrated by the Bland-Altman plots shown in Figures 4 and 5.

NP Area and ISI of Central and Montaged Images

Not surprisingly, the visible retinal area for montaged images was larger than that of central images: 221.7 ± 63.3 vs. $176.6 \pm 41.57 \text{ mm}^2$ ($P = 0.0087$), 822.8 ± 82.2 vs. $768.8 \pm 60.73 \text{ mm}^2$ ($P = 0.0133$), and 844.4 ± 99.10 vs. $777.1 \pm 59.82 \text{ mm}^2$ ($P = 0.007$) in the FPA, total area (TA) within the nonperfusion boundary (NPB), and TA of visible retina, respectively. Despite this, there was no difference in NP area or ISI for the various zones when comparing central and montaged images (Fig. 6).

Characteristics of Eyes With BRVO Compared With Eyes With CRVO

Table 2 compares the characteristics of eyes with BRVO and eyes with CRVO. Visual acuity of eyes with BRVO was significantly higher than that of eyes with CRVO (68.5 vs. 41 letters; $P = 0.0064$), and eyes with BRVO had significantly lower ISI for all zones except NPA (0.1607 vs. 0.2638; $P = 0.1276$). Both eyes with BRVO and those with CRVO demonstrated a gradual increase on ISI from the posterior

retina to the periphery, with the highest levels in the FPA ($P < 0.0001$).

Relationship Between BCVA and ISI From Different Retinal Zones

Figure 7 shows the correlation between BCVA and ISI derived from the central image. Significant correlations were found between visual acuity and ISI from different retinal zones, ranging from $r = -0.3825$ in PMA to $r = -0.584$ in FPA; in all cases, a higher ISI was associated with poorer vision. The GLM, adjusting for age and duration of disease (in year intervals), demonstrated that both PMA ($\beta = -1.059$; 95% confidence interval [CI]: -1.74 to -0.378) and FPA ($\beta = -0.505$; 95% CI: -0.988 to -0.021) were significant independent predictors of BCVA. No relationship was observed between ISI from the various rings/zones and the CMT (Table 3).

DISCUSSION

In this analysis of UWFFA images from RVO patients with ME in the WAVE trial, we compared the difference between central and montaged UWFFA images for calculating NP and ISI.

In comparing grading of the NP area for central and montaged images, ICCs were excellent with a high level of agreement between the two graders. We believed this high level of agreement was due to implementation of a standardized grading protocol, as well as implementation of a minimum size criterion (500 μm diameter) for a region to be considered as an area of NP. Of note, the differences between graders seemed to be greater on the montaged images than on the central images. It should be noted, however, that the montaged images did demonstrate and allow evaluation of a significantly larger FPA, TA within the NPB, and TA of total visible retina. The additionally visible peripheral areas, occasionally with blurred vessels in the far periphery, may have contributed to the slightly worse level of agreement.

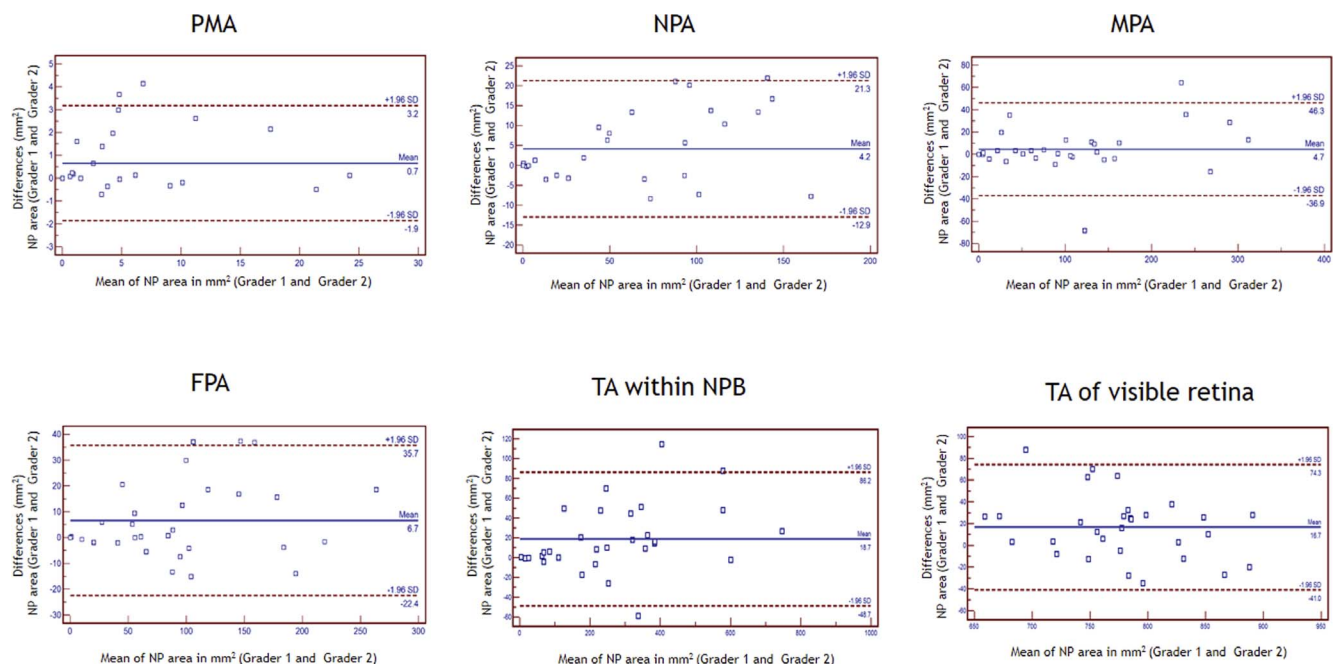


FIGURE 4. Bland-Altman plot illustrating the level of agreement between masked graders for determining nonperfusion area for central image. The high level of agreement between the two graders is illustrated by the Bland-Altman plots.

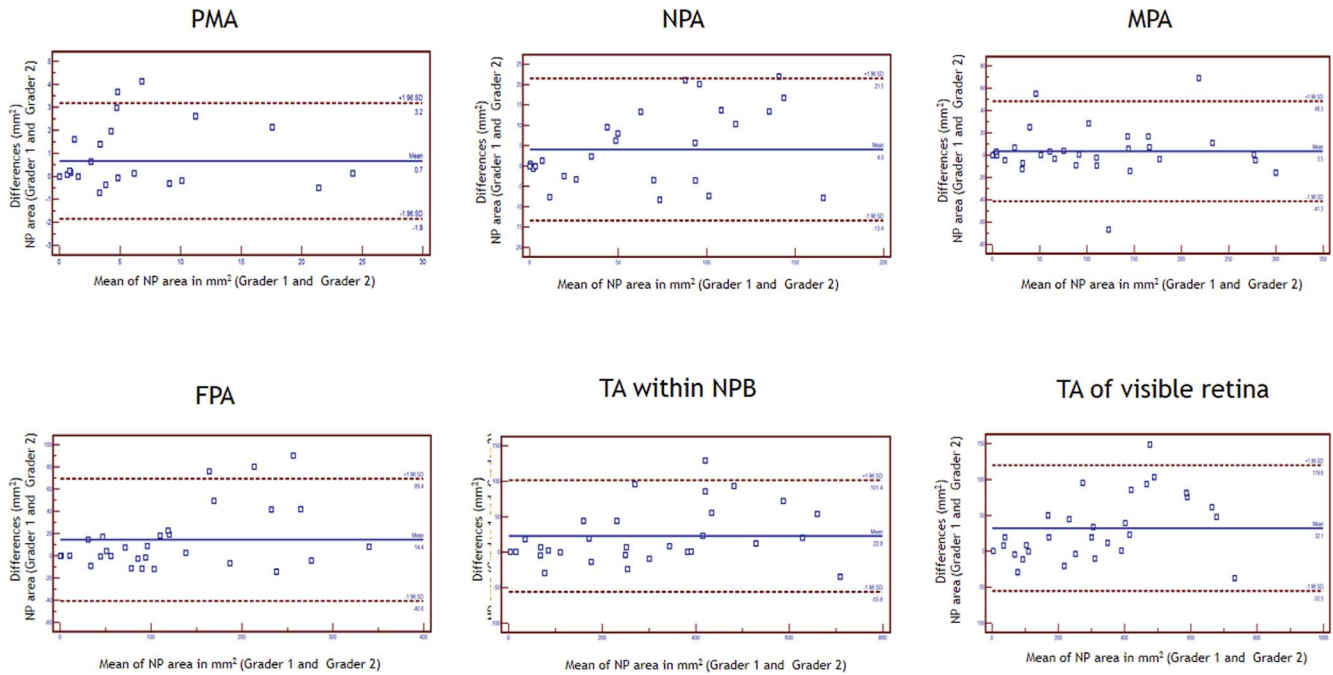


FIGURE 5. Bland-Altman plot illustrating the level of agreement between masked graders for determining nonperfusion area for montaged image. The high level of agreement between the two graders is also illustrated by the Bland-Altman plots.

Despite visualizing a significantly greater amount of retina, there was no significant difference between the single central image and montaged images with respect to NP area and ISI. The lack of difference in ISI is perhaps not surprising as it is a ratio based on the visible retina and thus may adjust for

differences in visible retina between central and montaged images. The lack of difference in NP area, however, suggests that much of the additional retina revealed by montaged images is either normal (physiologic) nonperfused retina or that ischemia from RVO does not significantly affect these regions.

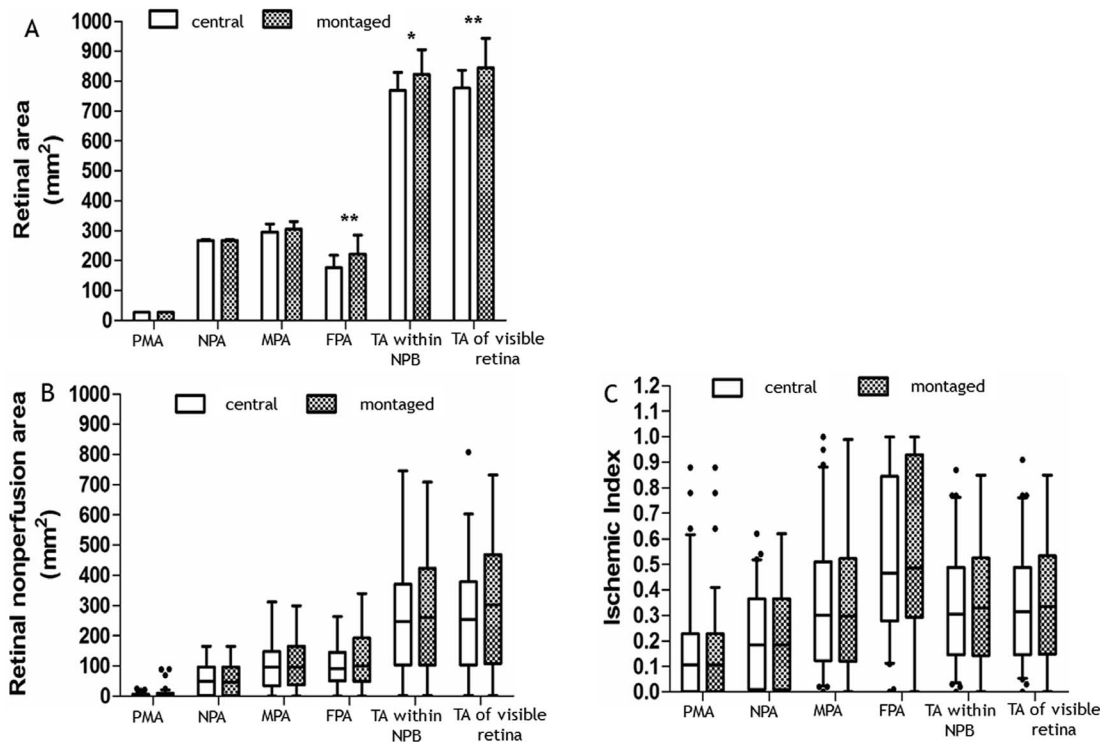


FIGURE 6. Comparison of total area of visible retina (A), retinal nonperfusion area (B), and ischemic index (C) for central and montaged image. The boxes show the median and 25% and 75% confidence intervals (*lower and upper quartiles*). The whiskers extend to what could be considered the 95% confidence interval. Outliers and extreme values are represented by dots beyond the whiskers. All differences from groups between central and montaged images are nonsignificant unless otherwise indicated, * $P < 0.05$, ** $P < 0.01$.

TABLE 2. Demographic Characteristics of Eyes With Branch Retinal Vein Occlusion Compared With Eyes with Central Retinal Vein Occlusion

Characteristic	BRVO (n = 14)	CRVO (n = 16)	P Value
Age, y	63 (26.75)	63.5 (32.75)	0.9502
Male sex	7 (50)	8 (50)	1
Duration, y	1 (2.5)	2 (3.75)	0.1676
BCVA, Snellen equivalent letters	68.5 (10.75)	41 (32)	0.0064
CMT, μm	433.5 (229.3)	517 (305.3)	0.5194
ISI of PMA	0.035 (0.1325)	0.16 (0.3775)	0.049
ISI of NPA	0.09 (0.335)	0.25 (0.3175)	0.1276
ISI of MPA	0.185 (0.2225)	0.46 (0.47)	0.0036
ISI of FPA	0.275 (0.2025)	0.805 (0.4425)	<0.0001
ISI of TA within NPB	0.19 (0.2225)	0.44 (0.3475)	0.0006
ISI of TA of visible retina	0.19 (0.22)	0.4445 (0.3325)	0.0005

Data are number (%) or median (interquartile range), unless otherwise indicated.

Regardless, the lack of difference would suggest that the time and expense to acquire steered images and generate montages may not be necessary for evaluation of NP in eyes with RVO.

We observed that the area of NP increased from the posterior pole to the periphery, in both BRVO and CRVO eyes, with the greatest extent of NP in the FPA (Table 2). Of note, this is in contrast to DR eyes, where more DR lesions and

nonperfusion are present in the MPR and then progress posteriorly with increasing disease severity.¹⁴ Similar to our findings, Prasad et al.¹⁵ also observed that areas of NP peripheral/anterior to the equator were at least twice as extensive as NP posterior to the equator. Interestingly, they also observed that untreated NP anterior to the globe equator was significantly associated with ME. Tomomatsu et al.¹⁶ and Singer et al.¹⁷ reported that TRP to these NP areas following intravitreal bevacizumab injection reduced the severity of recurrent ME compared with intravitreal bevacizumab injection alone.

It should be noted, however, that in our present study, we did not find any association between ISI from the various zones and CMT. There are several possible explanations for this observation. First, it is possible that only a small amount of retinal ischemia is necessary to trigger the production of VEGF and other cytokines and ISI is a not sensitive enough biomarker for this process. The observation that many RVO eyes have no significant areas of NP but still demonstrate ME would appear to support this argument. Second, systemic factors such as microvascular damage from uncontrolled hypertension, diabetes, and hyperlipidemia may decrease the threshold for the development of ME. Third, the inclusion criteria for the WAVE trial may have created a bias. All of the subjects in WAVE had recurrent or persistent edema and many eyes had a very long duration of disease and had been treated with multiple intravitreal injections. Thus, some of the cystoid changes observed in these individuals may have been degenerative and a reflection of the disease chronicity.¹⁸ This may also partially explain why the addition of TRP to ranibizumab resulted in no long-term benefit in BCVA, resolution of edema, or the number of ranibizumab injections required.¹⁹

Multivariable regression analysis indicated two significant predictors of BCVA in this group of RVO patients: a higher ISI in either the PMA or FPA was associated with poorer visual

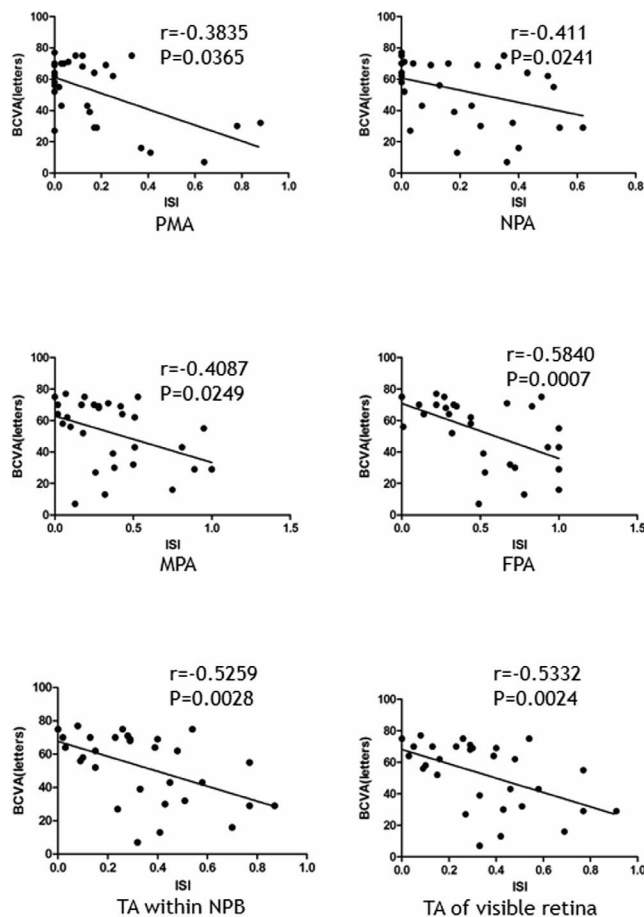


FIGURE 7. Relationship between BCVA and ISI from different retinal zones. In patients with retinal vein occlusion, scatterplots show relationships between visual acuity and ischemic index for PMA (top left), NPA (top right), MPA (middle left), FPA (middle right), and TA within normal perfusion boundary (bottom left) and TA of visible retina (bottom right) in central images.

TABLE 3. Correlation of Ischemic Index and Central Macular Thickness

Variable	Spearman r (95% Confidence Interval)	P
PMA	0.2021 (-0.1815 to 0.5323)	0.2841
NPA	0.0344 (-0.3399 to 0.3993)	0.8568
MPA	-0.0895 (-0.4448 to 0.2902)	0.6383
FPA	0.0301 (-0.3437 to 0.3957)	0.8745
TA within NPB	-0.0013 (-0.3712 to 0.3689)	0.9944
TA of visible retina	0.0147 (-0.3573 to 0.3826)	0.9386

Values of P (two-tailed) <0.05 were considered statistically significant.

acuity. According to our common perception, the progress of RVO varies by the site and degree of occlusion (ischemic or nonischemic). In general, more-distal RVO with less occlusion has a better prognosis than more-proximal RVO with greater ischemia.²⁰ As the PMA is in close proximity, it is not surprising that this could be associated with more associated vascular leakage and more associated NP affecting the adjacent fovea. The fact that the NP in the FPA was an important predictor of vision is of interest. Although the FPA is a great distance from the fovea, the far peripheral retina as defined in this study covers a much larger area than the PMA. The much larger amount of ischemic retina in the FPA compared with the PMA could presumably produce a much larger amount of VEGF, albeit at a greater distance from the fovea. Of course, VEGF is thought to play an important role in the pathogenesis of ME with RVO.²¹ Hypoxia causes increased expression of VEGF, which is a potent inducer of vascular permeability. The apparent relevance of NP in the FPA to the macula would appear to argue for a sound rationale for the TRP approach being evaluated in the WAVE trial.

Our study has several limitations that should be considered when assessing our results. First, to generate our measurements, we assumed a default axial length of 24 mm for all eyes as axial length was not collected in this study. However, the mean spherical equivalent was -0.10 D, and it is unlikely that any patient had extremely long or short axial lengths. Second, the sample size was relatively small and thus not powered to find small effects. For example, although age, duration of disease, and CMT have all been suggested to predict BCVA in previous studies,¹⁸ we found no relationship between these factors and vision in WAVE. A third limitation was that we did not evaluate foveal OCT features with BCVA and peripheral nonperfusion. The relationship between vision and OCT features in the setting of macular edema, however, has been evaluated in previous publications^{22,23} and was not the focus of this study. Third, the RVO population recruited into this study was required to have evidence of ischemia and to have persistent/recurrent ME; as such, our findings may not be applicable to the general population of those with RVO. Fourth, the NP measurements were based on manual segmentation and thus not immediately applicable to clinical practice. Automated software for measuring NP, however, is in development.

Our study also has several strengths, including data collection in a prospective clinical trial, a standardized acquisition and grading protocol, use of expert reading center graders, and use of stereographic projection software to generate precise measurements.

In summary, the findings from our study suggest that a single central UWFFA image may be sufficient to accurately evaluate peripheral NP in eyes with RVO. Both PMA and FPA appear to be significant predictors of visual acuity in eyes with RVO, highlighting the importance of peripheral NP in the disease process.

Acknowledgments

The authors thank Na Zeng, PhD, and Yuanyuan Kong, PhD (Clinical Epidemiology and EBM Center, Beijing Friendship Hospital, Capital Medical University; National Clinical Research Center for Digestive Disease, Beijing, China) for providing critical discussions and statistical analysis for our study and revision of the final manuscript.

Supported by a research grant from Genentech, Inc, South San Francisco, California, United States.

Disclosure: **K. Wang**, None; **K. Ghasemi Falavarjani**, None; **M.G. Nittala**, None; **M. Sagong**, None; **C.C. Wykoff**, None; **J. van Hemert**, Optos (E); **M. Ip**, None; **S.R. Sadda**, Optos (C, F),

Carl Zeiss Medic, (C, F), Centervue, (C, F), Heidelberg Engineering (F), Topcon Medical Systems, (F), Nidek (F)

References

1. Ho M, Liu DT, Lam DS, Jonas JB. Retinal vein occlusions, from basics to the latest treatment. *Retina*. 2016;36:432-448.
2. Singer M, Tan CS, Bell D, Sadda SR. Area of peripheral retinal nonperfusion and treatment response in branch and central retinal vein occlusion. *Retina*. 2014;34:1736-1742.
3. Tsui I, Kaines A, Havunjian MA, et al. Ischemic index and neovascularization in central retinal vein occlusion. *Retina*. 2011;31:105-110.
4. Tan CS, Chew MC, van Hemert J, Singer MA, Bell D, Sadda SR. Measuring the precise area of peripheral retinal non-perfusion using ultra-widefield imaging and its correlation with the ischaemic index. *Br J Ophthalmol*. 2016;100:235-239.
5. Ghasemi Falavarjani K, Wang K, Khadamy J, Sadda SR. Ultra-wide-field imaging in diabetic retinopathy: an overview. *J Curr Ophthalmol*. 2016;28:57-60.
6. Sagong M, van Hemert J, Olmos de Koo LC, Barnett C, Sadda SR. Assessment of accuracy and precision of quantification of ultra-widefield images. *Ophthalmology*. 2015;122:864-866.
7. Patel RD, Messner LV, Teitelbaum B, Michel KA, Hariprasad SM. Characterization of ischemic index using ultra-widefield fluorescein angiography in patients with focal and diffuse recalcitrant diabetic macular edema. *Am J Ophthalmol*. 2013;155:1038-1044.
8. Wessel MM, Nair N, Aaker GD, Ehrlich JR, D'Amico DJ, Kiss S. Peripheral retinal ischaemia, as evaluated by ultra-widefield fluorescein angiography, is associated with diabetic macular oedema. *Br J Ophthalmol*. 2012;96:694-698.
9. Sim DA, Keane PA, Rajendram R, et al. Patterns of peripheral retinal and central macula ischemia in diabetic retinopathy as evaluated by ultra-widefield fluorescein angiography. *Am J Ophthalmol*. 2014;158:144-153.
10. Singer M, Sagong M, van Hemert J, Kuehlewein L, Bell D, Sadda SR. Ultra-widefield imaging of the peripheral retinal vasculature in normal subjects. *Ophthalmology*. 2016;123:1053-1059.
11. Dubis AM, Hansen BR, Cooper RE, Beringer J, Dubra A, Carroll J. Relationship between the foveal avascular zone and foveal pit morphology. *Invest Ophthalmol Vis Sci*. 2012;53:1628-1636.
12. Blodi BA, Domalpally A, Scott IU, et al. Standard Care vs Corticosteroid for Retinal Vein Occlusion (SCORE) Study system for evaluation of stereoscopic color fundus photographs and fluorescein angiograms: SCORE Study Report 9. *Arch Ophthalmol*. 2010;128:1140-1145.
13. Nelder JA, Wedderburn RWM. Generalized linear models. *J R Stat Soc Ser A*. 1972;135:370-384.
14. Shimizu K, Kobayashi Y, Muraoka K. Midperipheral fundus involvement in diabetic retinopathy. *Ophthalmology*. 1981;88:601-612.
15. Prasad PS, Oliver SC, Coffee RE, Hubschman JP, Schwartz SD. Ultra wide-field angiographic characteristics of branch retinal and hemicentral retinal vein occlusion. *Ophthalmology*. 2010;117:780-784.
16. Tomomatsu Y, Tomomatsu T, Takamura Y, et al. Comparative study of combined bevacizumab/targeted photocoagulation vs bevacizumab alone for macular oedema in ischaemic branch retinal vein occlusions. *Acta Ophthalmol*. 2016;94:e225-e230.
17. Singer MA, Tan CS, Surapaneni KR, Sadda SR. Targeted photocoagulation of peripheral ischemia to treat rebound edema. *Clin Ophthalmol*. 2015;9:337-341.

18. Scott IU, VanVeldhuisen PC, Oden NL, et al. Baseline predictors of visual acuity and retinal thickness outcomes in patients with retinal vein occlusion: Standard Care Versus Corticosteroid for REtinal Vein Occlusion Study report 10. *Ophthalmology*. 2011;118:345-352.
19. Campochiaro PA, Hafiz G, Mir TA, et al. Scatter photocoagulation does not reduce macular edema or treatment burden in patients with retinal vein occlusion: the RELATE trial. *Ophthalmology*. 2015;122:1426-1437.
20. Pulido JS, Flaxel CJ, Adelman RA, Hyman L, Folk JC, Olsen TW. Retinal Vein Occlusions Preferred Practice Pattern® guidelines. *Ophthalmology*. 2016;123:182-208.
21. Campochiaro PA, Sophie R, Pearlman J, et al. Long-term outcomes in patients with retinal vein occlusion treated with ranibizumab: the RETAIN study. *Ophthalmology*. 2014;121:209-219.
22. Liu H, Li S, Zhang Z, Shen J. Predicting the visual acuity for retinal vein occlusion after ranibizumab therapy with an original ranking for macular microstructure. *Exp Ther Med*. 2018;15:890-896.
23. Kim HJ, Yoon HG, Kim ST. Correlation between macular ganglion cell-inner plexiform layer thickness and visual acuity after resolution of the macular edema secondary to central retinal vein occlusion. *Int J Ophthalmol*. 2018;11:256-261.